

On the equivalence of vapor-deposited and melt-quenched glasses

Cite as: J. Chem. Phys. **152**, 164504 (2020); <https://doi.org/10.1063/5.0006590>

Submitted: 05 March 2020 . Accepted: 07 April 2020 . Published Online: 23 April 2020

Zhe Wang, Tao Du, N. M. Anoop Krishnan, Morten M. Smedskjaer, and Mathieu Bauchy 



View Online



Export Citation



CrossMark

ARTICLES YOU MAY BE INTERESTED IN

[Configurational entropy of glass-forming liquids](#)

The Journal of Chemical Physics **150**, 160902 (2019); <https://doi.org/10.1063/1.5091961>

[X-ray and neutron scattering measurements of ordering in a \$\text{Cu}_{46}\text{Zr}_{54}\$ liquid](#)

The Journal of Chemical Physics **152**, 164503 (2020); <https://doi.org/10.1063/5.0003816>

[Can the glass transition be explained without a growing static length scale?](#)

The Journal of Chemical Physics **150**, 094501 (2019); <https://doi.org/10.1063/1.5086509>

Lock-in Amplifiers
up to 600 MHz



On the equivalence of vapor-deposited and melt-quenched glasses

Cite as: J. Chem. Phys. 152, 164504 (2020); doi: 10.1063/5.0006590

Submitted: 5 March 2020 • Accepted: 7 April 2020 •

Published Online: 23 April 2020



View Online



Export Citation



CrossMark

Zhe Wang,¹ Tao Du,^{1,2} N. M. Anoop Krishnan,^{3,4} Morten M. Smedskjaer,⁵ and Mathieu Bauchy^{1,a)} 

AFFILIATIONS

¹Physics of Amorphous and Inorganic Solids Laboratory (PARISlab), Department of Civil and Environmental Engineering, University of California, Los Angeles, California 90095, USA

²School of Civil Engineering, Harbin Institute of Technology, 150090 Harbin, China

³Department of Civil Engineering, Indian Institute of Technology Delhi, Hauz Khas, New Delhi 110016, India

⁴Department of Materials Science and Engineering, Indian Institute of Technology Delhi, Hauz Khas, New Delhi 110016, India

⁵Department of Chemistry and Bioscience, Aalborg University, 9220 Aalborg, Denmark

^{a)}Author to whom correspondence should be addressed: bauchy@ucla.edu. URL: <http://www.lab-paris.com>

ABSTRACT

Vapor deposition can yield glasses that are more stable than those obtained by the traditional melt-quenching route. However, it remains unclear whether vapor-deposited glasses are “allowable” or “forbidden,” that is, if they are equivalent to glasses formed by cooling extremely slowly a liquid or if they differ in nature from melt-quenched glasses. Here, based on reactive molecular dynamics simulation of silica glasses, we demonstrate that the allowable or forbidden nature of vapor-deposited glasses depends on the temperature of the substrate and, in turn, is found to be encoded in their medium-range order structure.

Published under license by AIP Publishing. <https://doi.org/10.1063/5.0006590>

I. INTRODUCTION

If quenched fast enough, liquids can avoid crystallization and remain in the metastable supercooled liquid state.¹ At the glass transition, the relaxation time eventually exceeds the observation time—so that melts experience a kinetic arrest and enter the out-of-equilibrium glassy state.^{2,3} As out-of-equilibrium phases, the structure and properties of glasses depend on their history. In particular, the use of lower cooling rates results in the formation of more stable glasses that occupy lower states in the energy landscape.¹ As an alternative route to melt-quenching, vapor deposition can yield ultrastable glasses^{4,5}—the degree of stability depending on the substrate temperature and deposition rate.^{4,6–9} The ultrastable nature of vapor-deposited glasses has been suggested to result from the enhanced mobility of the atoms at the surface of the deposited glass as compared with those in the bulk, thereby allowing deposited glasses to access lower energy states in an accelerated fashion.^{10,11} However, it remains unclear whether ultrastable vapor-deposited glasses are *allowable* (i.e., equivalent to glasses formed with a very slow cooling rate) or *forbidden* (i.e., glasses that cannot be formed via any thermal route).¹²

Here, based on reactive molecular dynamics (MD) simulations, we simulate and compare a series of (i) vapor-deposited SiO₂ glasses associated with varying substrate temperatures and (ii) melt-quenched SiO₂ freestanding films—so that all these systems exhibit a free surface and, hence, only differ from each other by their method of synthesis (i.e., vapor deposition vs melt-quenching). The fact of considering melt-quenched freestanding films rather than bulk glasses allows us to filter out the effect of the surface in our comparison between vapor-deposited and melt-quenched glasses.^{10,13} Importantly, we demonstrate that vapor-deposited glasses are allowable in the case of high substrate temperatures, but forbidden for low substrate temperatures. We find that the forbidden nature of glasses deposited on low-temperature substrates is primarily encoded in their ring size distribution.

II. METHODS

To establish our conclusions, we conduct a series of MD simulations of vapor-deposited SiO₂ glasses. A tetragonal simulation box with a height of 75 Å (*z*-axis) and lateral dimensions of 28 Å

(x - and y -axis) is first created. The box is surrounded by two reflective walls on the top and bottom, while periodic boundary conditions are imposed laterally. A melt-quenched silica glass with a vertical thickness of 14 Å is placed at the bottom and serves as the substrate. The deposition process is then simulated by iteratively placing new SiO₂ molecules at the top of the box ($70 \text{ Å} < z < 75 \text{ Å}$) with a downward velocity of 0.02 Å/fs, wherein the initial horizontal position of inserted molecules is randomly chosen.^{7,10} We find that a deposition rate of 0.5 SiO₂/ps is slow enough to ensure a fair convergence of the potential energy of the deposited glass (see the [supplementary material](#)). Hence, this deposition rate is kept constant in all simulations. The substrate temperature used herein ranges from 500 K to 3500 K—as we observe that, at higher temperature, the inserted particles remain in a gas phase and do not deposit on the substrate. The dynamics of all atoms is governed by a Langevin thermostat to model a Brownian dynamics during the deposition, wherein the temperature is controlled by adding some additional fictitious forces (friction and dispersion).¹⁴ We adopt this method since it has been shown to yield more stable vapor-deposited configurations than cases wherein the temperature of the vapor atoms is controlled by a Nosé–Hoover thermostat in the canonical ensemble (NVT).^{7,10} We use a damping factor of 50 fs and the rotational degrees of freedom are not thermostatted. The deposition process is continued until 512 SiO₂ molecules are deposited on the substrate, which results in the formation of a vapor-deposited glass that is about 35 Å high. The vapor-deposited configuration is eventually subjected to a zero-stress energy minimization using the conjugate gradient algorithm to obtain the inherent configuration.^{7,10,16} This energy minimization under constant stress aims to remove any residual stress in the atomic structure but does not affect the connectivity of the glasses.

To compare vapor-deposited to melt-quenched SiO₂ glasses, we simulate the formation of freestanding melt-quenched glassy silica films¹⁷—which allows us to isolate the effect of the synthesis method on their structure while maintaining the common presence of a free surface. First, initial configurations are created by randomly placing 512 SiO₂ molecules in a cube with lateral dimensions of 28 Å and periodic boundary conditions, while ensuring the absence of any unrealistic overlap. Second, the simulation boxes are fixed to 70 Å in the z -direction. Similar to the vapor deposition simulations, no periodic boundary conditions are applied along this direction and two reflective walls are placed on both ends of the simulation box. All systems are then relaxed at 3600 K and zero stress in the isothermal–isobaric ensemble (NPT) for 100 ps to ensure that they lose the memory of their initial configurations while, nevertheless, remaining a cohesive film. The obtained liquids are then subsequently quenched into glasses by linearly cooling the systems from 3600 K to 300 K under zero stress in the NPT ensemble. Varying cooling rates ranging from 10 000 down to 1 K/ps are used to generate glasses exhibiting varying fictive temperatures,¹⁸ i.e., differing thermal histories. All glasses are eventually subjected to a zero-stress energy minimization to access their inherent configuration.

Note that, to filter out the effects of the surface and substrate, we conduct all subsequent structural analyses on a subsection of the films that are far enough from the surface and substrate. The vertical extent of these domains (i.e., from $z = 10 \text{ Å}$ to 25 Å and $z = 10 \text{ Å}$ to 30 Å for the melt-quenched and vapor-deposited films,

respectively) is determined by plotting some vertical profiles of the average potential energy per atom as a function of z (see the [supplementary material](#)). In each case, structural data are averaged over six independent simulations for statistical purposes. To ensure a consistent comparison between vapor-deposited and melt-quenched glasses, all simulations are conducted with the same forcefield. We adopt the reactive ReaxFF potential parameterized by Fogarty *et al.*,¹⁹ with a time step of 0.5 fs. Importantly, ReaxFF can (i) account for charge transfers and dynamic formations of interatomic bonds,²⁰ (ii) handle coordination defects,^{20,21} and (iii) realistically describe the structure of glassy SiO₂.²² Thanks to these features, ReaxFF can properly describe both the vapor deposition and melt-quenching processes with a constant set of parameters.²³ All simulations are conducted with LAMMPS.²⁴

III. RESULTS AND DISCUSSION

We first assess the thermodynamic stability of the vapor-deposited glasses as a function of the substrate temperature. To this end, rather than relying on the total potential energy of the system, we compute the potential energy per Q⁴ Si atom (i.e., Si atom connected to four bridging oxygen atoms) to filter out the contribution of coordination defects and isolate the intrinsic thermodynamic stability of the network. [Figure 1](#) shows the inherent structure potential energy per Q⁴ Si atom in vapor-deposited glasses as a function of the substrate temperature. The results are compared with the inherent structure potential energy of a melt-quenched freestanding glassy film prepared with a cooling rate of 1 K/ps.^{22,25,26} Overall, we observe that the potential energy per Q⁴ Si atom in vapor-deposited glasses

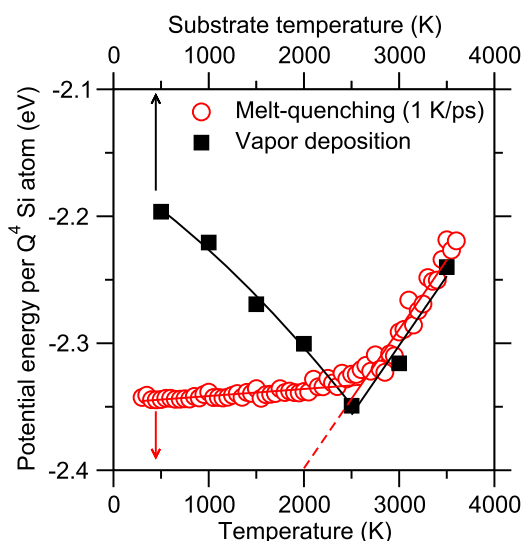


FIG. 1. Inherent structure average potential energy per Q⁴ Si atom in both (i) vapor-deposited glasses as a function of the temperature of the substrate and (ii) a melt-quenched glass prepared with a cooling rate of 1 K/ps as a function of temperature. In each case, the arrows point toward the relevant temperature to be considered. The solid lines are to guide the eye. The dashed line is an extrapolation of the supercooled liquid domain.

exhibits a “V-shape” dependence on the substrate temperature, in agreement with previous results obtained for a 2D model glass.^{4,6} The total potential energy per atom exhibits a similar trend (see the [supplementary material](#)). The most stable vapor-deposited glass is obtained for a substrate temperature of about 2500 K, which is slightly lower than the computed fictive temperature of the melt-quenched glass, that is, the temperature at which the energy exhibits a break in slope (see [Fig. 1](#))—note that both of these temperatures are here shifted toward higher values as compared to experiments due to the limited timescale accessible to MD simulations. This trend echoes previous simulation and experimental results.^{6,15} Notably, at the substrate temperature of 2500 K, the vapor-deposited glass is slightly more stable than the melt-quenched glass—although this observation is specific to the deposition and cooling rates used herein. Overall, these results highlight that the behaviors of realistic (e.g., SiO₂) and model (e.g., Lennard-Jones) vapor-deposited glasses appear to be governed by the same underlying physics.

We now investigate the origin of the high stability featured by vapor-deposited SiO₂ glasses at 2500 K (see [Fig. 1](#)). In line with results obtained for 2D model glasses,¹⁰ we suggest that the minimum of potential energy arises from a competition between thermodynamics and kinetics. To establish this picture, we explore the dynamics of the vapor-deposited glasses by computing the mean squared displacement (MSD) of the Si atoms as a function of temperature.^{15,27–29} All calculations are conducted in the *NVT* ensemble over a duration of 250 ps. As expected, the MSD exhibits three stages, that is, (i) a ballistic regime at short time (slope of 2 in the log–log scale), (ii) a cage-effect plateau at intermediate time, and (iii) a diffusive regime, which manifests itself by a slope of 1 in the log–log scale^{30,31} (see the inset of [Fig. 2](#) and the [supplementary material](#)). Notably, the dynamics of the surface atoms (i.e., within a 5 Å-thick region at the top of the sample) differs from those in the bulk. In detail, we find that the MSD of the surface atoms is systematically larger than in the bulk (see [Fig. 2](#))—albeit to a lesser

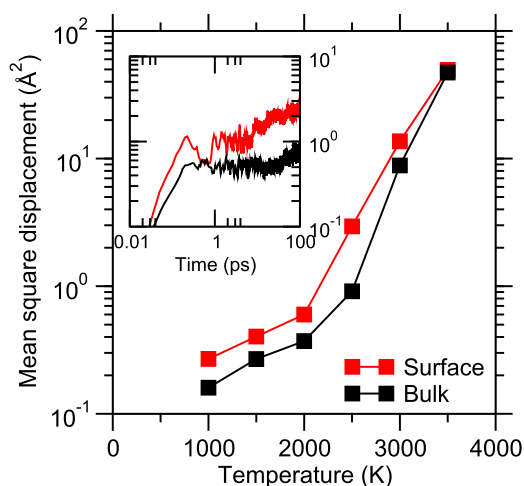


FIG. 2. Mean squared displacement (MSD) after 250 ps of dynamics of Si atoms located in the bulk or surface of vapor-deposited SiO₂ glasses as a function of temperature. The inset shows the MSD for bulk and surface Si atoms at 2500 K.

extent at higher temperature. We also observe that the duration of the cage effect is about one order of magnitude shorter at the surface than in the bulk (see the inset of [Fig. 2](#)). This likely arises from the fact that surface atoms are less constrained than bulk atoms³² and, hence, have access to additional relaxation channels in the energy landscape.³³

Based on these results, the V-shape of the potential energy can be rationalized as follows.¹⁰ At high temperature, the relaxation time of both vapor-deposited and melt-quenched systems is smaller than the observation time. Hence, both systems can reach the metastable equilibrium supercooled liquid state. As temperature decreases, lower-energy supercooled liquid states become more thermodynamically favored, so that both vapor-deposited and melt-quenched systems reach more stable positions in the energy landscape. However, at the vicinity of the glass transition, due to the kinetics slowdown, the relaxation time of bulk melt-quenched systems becomes longer than the observation time—so that they become out-of-equilibrium glasses and remain stuck in unstable positions in the energy landscape. In contrast, at constant observation time, vapor-deposited glasses relax faster than melt-quenched glasses, thanks to the faster kinetics of their surface atoms. Hence, vapor-deposited glasses remain in the metastable equilibrium supercooled liquid state down to lower temperatures (and, hence, reach more stable basins in the energy landscape) than melt-quenched glasses at constant observation time. However, as the substrate temperature continues to decrease, the increased slowdown in relaxation kinetics eventually prevents the atoms from relaxing toward low-energy states when they get deposited at the glass surface, which results in an increase in potential energy. Overall, the substrate temperature at which vapor-deposited glasses feature minimum potential energy is controlled by the competition between thermodynamics (i.e., increased thermodynamic propensity to relax toward lower-energy states as temperature decreases) and kinetics (i.e., decreased ability to reach such stable states as temperature decreases).

We now interrogate whether vapor-deposited glasses are forbidden or allowable. That is, do vapor-deposited glasses differ in nature from melt-quenched glasses or can they also be formed by melt-quenching with a given (slow) cooling rate? Specifically, can the increase in the potential energy of vapor-deposited glasses with low substrate temperature (see [Fig. 1](#)) be understood as an increase in fictive temperature? To answer this question, [Fig. 3](#) shows the inherent structure average potential energy as a function of the average Voronoi volume per Q⁴ Si atom in vapor-deposited glasses prepared with varying substrate temperature and melt-quenched freestanding glassy films prepared with cooling rates varying from 10 000 to 1 K/ps (i.e., varying fictive temperature).²⁵ Although the potential energy and volume do not uniquely characterize a glass,³⁴ the potential energy captures the degree of stability of a glass and, to the first order, largely depends on the short-range order, whereas the volume captures the overall compactness of the glass, which is strongly affected by the medium-range order.²⁵ As such, the energy-volume space shown in [Fig. 3](#) offers a convenient map to compare vapor-deposited and melt-quenched glasses.

We first focus on the melt-quenched freestanding glassy films. For the range of cooling rates considered herein (which remain significantly larger than in typical experiments¹⁷), the average Voronoi volume per Q⁴ Si atom decreases with the decrease in the cooling

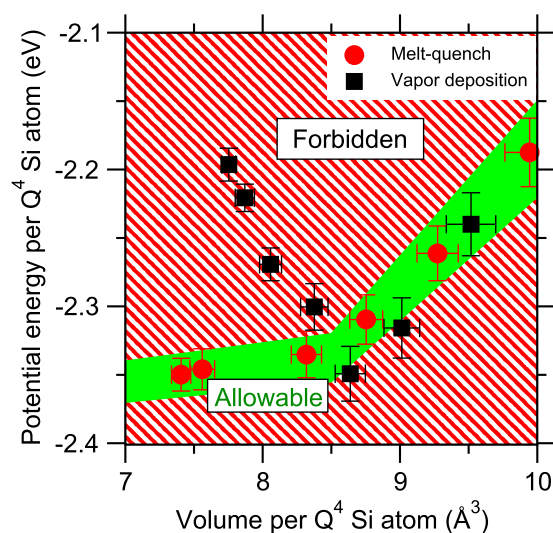


FIG. 3. Inherent structure average potential energy as a function of the average Voronoi volume per Q^4 Si atom in (i) vapor-deposited glasses prepared with varying substrate temperature and (ii) melt-quenched glasses prepared with varying cooling rates (i.e., varying fictive temperature). The green region is a rough indication of the range of “allowable” states, whereas other states are “forbidden.”

rate (i.e., the system becomes more optimally packed), while the average potential energy per Q^4 Si atom decreases and eventually plateaus (i.e., the system becomes more stable and achieves a lower fictive temperature).²⁵ These states define the range of allowable states that are accessible to melt-quenched glasses within the time scale accessible to our MD simulations (i.e., as roughly indicated by the green region in Fig. 3).

We now place our attention to the states occupied by vapor-deposited glasses in the energy-volume map. We find that, at high substrate temperature, vapor-deposited glasses are equivalent to hyperquenched melt-quenched glasses prepared with high cooling rates (see Fig. 3). This signals that, in this regime, vapor-deposited glasses are allowable and the increase in potential energy upon increasing substrate temperature can be understood in terms of an increase in fictive temperature. This echoes the fact that, in this range of temperature, both vapor-deposited and melt-quenched glasses are able to relax toward the same metastable equilibrium supercooled liquid state. In sharp contrast, at low substrate temperature, vapor-deposited glasses deviate from the states occupied by melt-quenched glasses in the energy-volume map (see Fig. 3). Namely, upon decreasing substrate temperature, the potential energy per Q^4 Si atom increases while the volume per Q^4 Si atom keeps decreasing. This indicates that, in this regime, the increase in potential energy exhibited by vapor-deposited glasses upon increasing substrate temperature cannot be understood in terms of an increase in fictive temperature—so that such vapor-deposited glasses are forbidden. These results demonstrate that the allowable vs forbidden nature of vapor-deposited glasses depends on the substrate temperature.

Finally, we investigate how the allowable vs forbidden nature of vapor-deposited glasses is encoded in their structure. Note that, in the following, to ensure a fair comparison between the atomic

structure of vapor-deposited and melt-quenched glassy films, we restrict the comparison to glasses having fairly similar potential energy (see Fig. 1 for a comparison between the energy of vapor-deposited and melt-quenched glasses). In detail, we conduct three distinct comparisons: (i) the “allowable” vapor-deposited associated with a substrate temperature of 3500 K is compared with a melt-quenched glassy film cooled at 10 000 K/ps, (ii) the “allowable” vapor-deposited associated with a substrate temperature of 2500 K is compared with a melt-quenched glassy film cooled at 1 K/ps, and (iii) the “forbidden” vapor-deposited associated with a substrate temperature of 500 K is compared with a melt-quenched glassy film cooled at 10 000 K/ps.

First, we find that regardless of the substrate temperatures, the Si–O partial pair distribution functions obtained from vapor-deposited and melt-quenched glasses match well with each other (see the supplementary material). Similarly, the O–Si–O intratetrahedral partial bond angle distributions do not reveal any notable differences between the short-range order structure of both glasses either (see the supplementary material). This may explain why vapor-deposited glasses have previously been assumed to be structurally similar to melt-quenched ones.¹⁰ The short-range order analysis being largely inconclusive, we change our focus to the medium-range order, which, in silicate glasses, is described by the ring size distribution^{35–38}—wherein a ring is defined as a closed path made of Si–O bonds in the network with a size being given by the number of Si atoms. All ring size distributions are computed using RINGS.³⁷

Figure 4 shows the ring size distribution of the three selected vapor-deposited glasses, which, in each case, is compared to that of their melt-quenched counterparts. We find that, as expected, all distributions are centered around 5–6 membered rings.³⁹ We first note that no significant difference is observed between the ring size distribution of the “allowable” vapor-deposited glasses (i.e., at high and intermediate substrate temperature) and that of their melt-quenched counterparts [see Figs. 4(b) and 4(c)]. However, in contrast, we observe that the ring size distribution of forbidden vapor-deposited glasses (i.e., prepared with low substrate temperatures) exhibit distinct features. In detail, we find that the ring size distribution of the forbidden vapor-deposited glass presents an excess of small rings (i.e., 4-membered rings and smaller) as compared to its melt-quenched counterpart, as well as in comparison to the other allowable vapor-deposited glasses [see Fig. 4(a)]. Such small rings have been shown to be topologically over-constrained and to constitute a signature of instability.^{35,39} Such instability manifests itself by a decrease in the average value of the intertetrahedral Si–O–Si angles (see the supplementary material), which echoes previous findings.³⁹

In turn, such small rings result in the formation of efficiently-packed structures—since small rings are associated with low diameters, whereas larger rings present more open structures.⁴⁰ As such, the existence of a large fraction of small rings explains why forbidden vapor-deposited glasses prepared with low substrate temperatures simultaneously exhibit high potential energy and high packing efficiency. Such small rings can be formed when atoms get randomly deposited at the surface of the glass—irrespective of the substrate temperature. However, due to their unstable nature, small rings are likely to quickly disappear as the surface atoms relax toward more stable configurations. However, the slowdown in relaxation

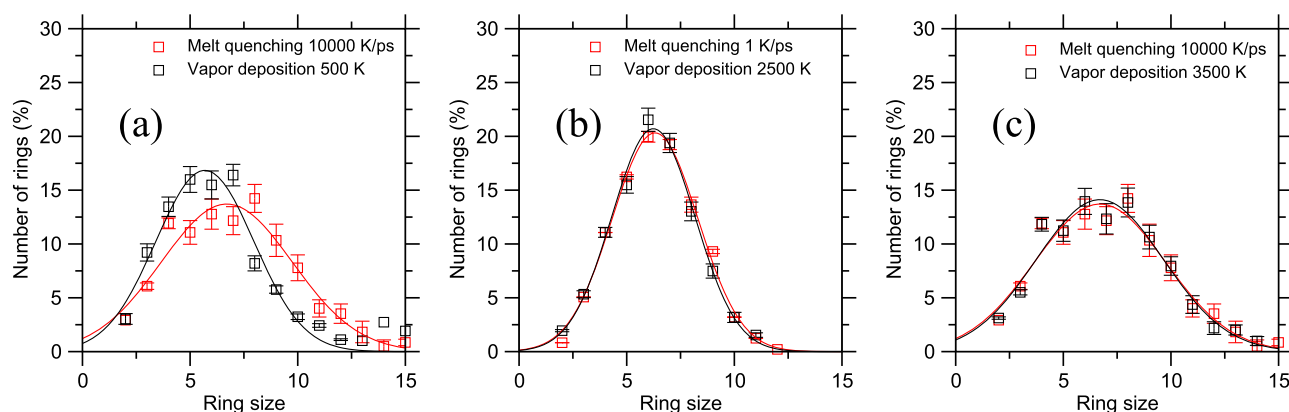


FIG. 4. Ring size distribution in vapor-deposited glasses prepared with a substrate temperature of (a) 500 K, (b) 2500 K, and (c) 3500 K. In each of these cases, the distributions are compared with those obtained in a melt-quenched glass presenting a molar potential energy that is comparable with that of the vapor-deposited glass (i.e., as obtained with a cooling rate of 10 000 K/ps, 1 K/ps, and 10 000 K/ps, respectively). The lines are to guide the eye.

kinetics experienced by vapor-deposited glasses prepared with low-temperature substrates prevents the efficient relaxation of such energetically unfavorable small rings.

We note that the excess of unusual small rings observed herein at low substrate temperatures echoes previous observations of local molecular anisotropy in vapor-deposited glasses.^{41–43} Indeed, in both cases, such unusual structural features (i.e., small rings in network glasses or anisotropic molecular orientation in molecular glasses) are formed at the glass surface upon deposition and, if relaxation is slow enough, remain trapped within the bulk after further deposition occurs. In both cases, the propensity to retain such unusual structural features frozen within the bulk increases as the deposition temperature becomes lower as compared to T_g due to the dramatic slowdown of the relaxation kinetics. In turn, when the deposition temperature exceeds T_g , the existence of fast relaxation modes prevents the accumulation and persistence of such defected structural features.

IV. CONCLUSIONS

Overall, these results highlight that the forbidden or allowable nature of vapor-deposited glasses depends on the temperature of the substrate used during deposition and is controlled by a competition between thermodynamics and kinetics—wherein thermodynamics drives the relaxation of vapor-deposited glasses toward allowable metastable supercooled liquids, whereas kinetics can prevent such relaxation and tend to freeze some unrealistic small ring defects formed during deposition that are otherwise virtually absent from allowable melt-quenched glasses. The fact that both the melt-quenched freestanding films and vapor-deposited glasses present a free surface ensures that differences in the structure and properties of melt-quenched and vapor-deposited glasses are not just a spurious consequence of the presence of a surface. More generally, these results suggest that the allowable vs forbidden nature of disordered networks is encoded in their medium-range (rather than short-range) order. These results also suggest that, in addition to being a promising route toward the synthesis of ultrastable

allowable glasses, vapor deposition offers an intriguing pathway toward the design of forbidden glasses that are not accessible to the melt-quench route and, hence, could exhibit unusual properties (e.g., enhanced mechanical properties and low propensity for relaxation).

SUPPLEMENTARY MATERIAL

We provide as [supplementary material](#) some atomic snapshots of the vapor-deposited glasses and some additional analyses (effects of the deposition rate, vertical profile of the atomic potential energy, short-range order analysis, and so on) to further support our simulations.

ACKNOWLEDGMENTS

This work was supported by the National Science Foundation under Grant No. 1928538. N.M.A.K. acknowledges some financial support provided by the Department of Science and Technology, India, under the INSPIRE faculty scheme (Grant No. DST/INSPIRE/04/2016/002774) and the DST SERB Early Career Award (No. ECR/2018/002228).

REFERENCES

- ¹P. G. Debenedetti and F. H. Stillinger, *Nature* **410**, 259 (2001).
- ²A. K. Varshneya, *Fundamentals of Inorganic Glasses* (Academic Press, Inc., 1993).
- ³E. D. Zanotto and J. C. Mauro, *J. Non-Cryst. Solids* **471**, 490 (2017).
- ⁴S. F. Swallen, K. L. Kearns, M. K. Mapes, Y. S. Kim, R. J. McMahon, M. D. Ediger, T. Wu, L. Yu, and S. Satija, *Science* **315**, 353 (2007).
- ⁵M. D. Ediger, *J. Chem. Phys.* **147**, 210901 (2017).
- ⁶K. L. Kearns, S. F. Swallen, M. D. Ediger, T. Wu, and L. Yu, *J. Chem. Phys.* **127**, 154702 (2007).
- ⁷S. Singh, M. D. Ediger, and J. J. de Pablo, *Nat. Mater.* **12**, 139 (2013).
- ⁸K. L. Kearns, S. F. Swallen, M. D. Ediger, T. Wu, Y. Sun, and L. Yu, *J. Phys. Chem. B* **112**, 4934 (2008).
- ⁹S. S. Dalal, D. M. Walters, I. Lyubimov, J. J. de Pablo, and M. D. Ediger, *Proc. Natl. Acad. Sci. U. S. A.* **112**, 4227 (2015).

- ¹⁰D. R. Reid, I. Lyubimov, M. D. Ediger, and J. J. de Pablo, *Nat. Commun.* **7**, 13062 (2016).
- ¹¹J. R. Dutcher and M. D. Ediger, *Science* **319**, 577 (2008).
- ¹²J. C. Mauro and R. J. Loucks, *J. Non-Cryst. Solids* **355**, 676 (2009).
- ¹³L. Berthier, P. Charbonneau, E. Flenner, and F. Zamponi, *Phys. Rev. Lett.* **119**, 188002 (2017).
- ¹⁴T. Schneider and E. Stoll, *Phys. Rev. B* **17**, 1302 (1978).
- ¹⁵I. Lyubimov, M. D. Ediger, and J. J. de Pablo, *J. Chem. Phys.* **139**, 144505 (2013).
- ¹⁶E. Bitzek, P. Koskinen, F. Gähler, M. Moseler, and P. Gumbsch, *Phys. Rev. Lett.* **97**, 170201 (2006).
- ¹⁷X. Li, W. Song, K. Yang, N. M. A. Krishnan, B. Wang, M. M. Smedskjaer, J. C. Mauro, G. Sant, M. Balonis, and M. Bauchy, *J. Chem. Phys.* **147**, 074501 (2017).
- ¹⁸Z. Liu, Y. Hu, X. Li, W. Song, S. Goyal, M. Micoulaut, and M. Bauchy, *Phys. Rev. B* **98**, 104205 (2018).
- ¹⁹J. C. Fogarty, H. M. Aktulga, A. Y. Grama, A. C. T. van Duin, and S. A. Pandit, *J. Chem. Phys.* **132**, 174704 (2010).
- ²⁰A. C. T. van Duin, S. Dasgupta, F. Lorant, and W. A. Goddard, *J. Phys. Chem. A* **105**, 9396 (2001).
- ²¹H. Aktulga, J. Fogarty, S. Pandit, and A. Grama, *Parallel Comput.* **38**, 245 (2012).
- ²²Y. Yu, B. Wang, M. Wang, G. Sant, and M. Bauchy, *J. Non-Cryst. Solids* **443**, 148 (2016).
- ²³L. Meng, Q. Sun, J. Wang, and F. Ding, *J. Phys. Chem. C* **116**, 6097 (2012).
- ²⁴S. Plimpton, *J. Comput. Phys.* **117**, 1 (1995).
- ²⁵N. M. A. Krishnan, B. Wang, Y. Yu, Y. Le Pape, G. Sant, and M. Bauchy, *Phys. Rev. X* **7**, 031019 (2017).
- ²⁶N. M. A. Krishnan, B. Wang, Y. Le Pape, G. Sant, and M. Bauchy, *Phys. Rev. Mater.* **1**, 053405 (2017).
- ²⁷C. Donati, S. C. Glotzer, P. H. Poole, W. Kob, and S. J. Plimpton, *Phys. Rev. E* **60**, 3107 (1999).
- ²⁸P.-H. Lin, I. Lyubimov, L. Yu, M. D. Ediger, and J. J. de Pablo, *J. Chem. Phys.* **140**, 204504 (2014).
- ²⁹G. Sun, S. Saw, I. Douglass, and P. Harrowell, *Phys. Rev. Lett.* **119**, 245501 (2017).
- ³⁰M. Bauchy, B. Guillot, M. Micoulaut, and N. Sator, *Chem. Geol.* **346**, 47 (2013).
- ³¹M. Bauchy and M. Micoulaut, *Phys. Rev. B* **83**, 184118 (2011).
- ³²Y. Yu, N. M. A. Krishnan, M. M. Smedskjaer, G. Sant, and M. Bauchy, *J. Chem. Phys.* **148**, 074503 (2018).
- ³³C. W. Brian and L. Yu, *J. Phys. Chem. A* **117**, 13303 (2013).
- ³⁴M. M. Smedskjaer, M. Bauchy, J. C. Mauro, S. J. Rzoska, and M. Bockowski, *J. Chem. Phys.* **143**, 164505 (2015).
- ³⁵M. Micoulaut and J. C. Phillips, *Phys. Rev. B* **67**, 104204 (2003).
- ³⁶A. E. Geissberger and F. L. Galeener, *Phys. Rev. B* **28**, 3266 (1983).
- ³⁷S. Le Roux and P. Jund, *Comput. Mater. Sci.* **49**, 70 (2010).
- ³⁸S. R. Elliott, *Nature* **354**, 445 (1991).
- ³⁹W. Song, X. Li, B. Wang, N. M. Anoop Krishnan, S. Goyal, M. M. Smedskjaer, J. C. Mauro, C. G. Hoover, and M. Bauchy, *Appl. Phys. Lett.* **114**, 233703 (2019).
- ⁴⁰Y. Shi, J. Neufeind, D. Ma, K. Page, L. A. Lamberson, N. J. Smith, A. Tandia, and A. P. Song, *J. Non-Cryst. Solids* **516**, 71 (2019).
- ⁴¹S. S. Dalal and M. D. Ediger, *J. Phys. Chem. Lett.* **3**, 1229–1233 (2012).
- ⁴²J. Jiang, D. M. Walters, D. Zhou, and M. D. Ediger, *Soft Matter* **12**, 3265–3270 (2016).
- ⁴³I. Lyubimov, L. Antony, D. M. Walters, D. Rodney, M. D. Ediger, and J. J. de Pablo, *J. Chem. Phys.* **143**, 094502 (2015).